



Atomic rheology analysis of the external magnetic field effects on nanofluid in non-ideal microchannel via molecular dynamic method

Yuanzhou Zheng^{1,2} · Xinzhu Zhang^{1,2} · Mohammad Nouri³ · Ali Amini³ · Arash Karimipour⁴ · Maboud Hekmatifar^{5,6} · Roozbeh Sabetvand⁷ · Qooyen Ngooyen³ · Aliakbar Karimipour⁸

Received: 25 March 2020 / Accepted: 17 August 2020 / Published online: 15 September 2020
© Akadémiai Kiadó, Budapest, Hungary 2020

Abstract

In the present study, the molecular dynamics method is used to probe the aggregation phenomenon of hybrid nanoparticle within platinum microchannel with pyramidal barriers. In molecular dynamics simulations, argon atoms are described as base fluid particles and for the interaction between these atoms, we use Lennard-Jones potential, while the platinum–platinum and Al₂O₃ nanoparticles interactions are simulated applying the embedded atom method force field. To analyze the achieved simulation results, some physical parameters such as potential energy, temperature, and distance of nanoparticles center of mass are calculated. The results show external magnetic field decrease the aggregation phenomenon in nanoparticles. Numerically, by adding external magnetic field to simulation box, the COM distance of nanoparticles reaches to 2.7 Å and the aggregation time of nanoparticles changes from 1.7 to 2.3 ns. These appropriate effects of external magnetic field from our computational study can be used in the design of heat transfer applications.

Keywords Hybrid · Molecular dynamic simulation · Aggregation · Microchannel

Introduction

A nanofluid can be defined as a fluid having nanosized particles, which is named nanoparticles. The colloidal suspensions of nanoparticles are designed by these fluids [1, 2]. Oxides, metals, silicon carbides, and carbon nanotubes are the components of nanoparticles, which are used in nanofluids. Further, oil, ethylene glycol, and water are some of the common fluids [3]. Innovative features of nanofluids cause

them potentially effective for lots of uses in heat transmitting, such as fuel cells, microelectronics, pharmaceutical procedures, and hybrid-powered engines, electronic cooling systems, household fridges, chillers, heat exchangers, in machining, grinding equipment and in boiler flue gas temperature decreasing [4, 5]. One of the most importance of these structures is good thermal conductivity of them [6–8]. In comparison with the common fluids, they indicate better thermic power of conducting and convicted heat transmitting

✉ Arash Karimipour
arashkarimipour@tdtu.edu.vn

Aliakbar Karimipour
aliakbarkarimipour@duytan.edu.vn

¹ Engineering Research Center of Fujian University for Marine Intelligent Ship Equipment, Minjiang University, Fuzhou 350108, China

² School of Mechanical, Materials, Mechatronic and Biomedical Engineering, University of Wollongong, Wollongong, NSW 2522, Australia

³ Department of Mechanical Engineering, Najafabad Branch, Islamic Azad University, Najafabad, Iran

⁴ Department of Mechanical Engineering, Najafabad branch, Islamic Azad University, Najafabad, Iran

⁵ Young Researchers and Elite Club, Khomeinishahr Branch, Islamic Azad University, Khomeinishahr, Iran

⁶ Department of Mechanical Engineering, Khomeinishahr Branch, Islamic Azad University, Khomeinishahr, Iran

⁷ Department of Energy Engineering and Physics, Faculty of Condensed Matter Physics, Amirkabir University of Technology, Tehran, Iran

⁸ Institute of Research and Development, Duy Tan University, Da Nang 550000, Vietnam

efficiency [9]. So various types of these nanostructures are used in many reality applications for achieving high rate of thermal manner of optimized structures with nanofluids [10–13]. Reason for being critical about determining the appropriateness to convective heat transferring uses is a rise in knowledge of nanofluids rheological behavior [14, 15]. Unlike many benefits of nanofluids, some adverse phenomenon can disrupt their properties. One of the most important inappropriate phenomena is the aggregation of nanoparticles in nanofluid structures. Previously, some researchers investigated the effect of both nanoparticle size and aggregation upon viscosity [16–18]. Nkurikiyimfura et al. [19] proposed that nanoparticle accumulation may cause increasing thermal conductivity for nanofluids. The transfer electron micrograph picture of copper–water nanofluids was observed by Xuan et al. [20] in experiments. Not only did they fulfill a simulation of nanoparticle aggregation, but they also regarded that Brownian motion resulted in abnormal movement of nanoparticles. Murshed et al. [21] made nanofluids ready by various volume fractions of TiO₂ nanoparticles. By the study of previous reports in nanofluid structures [22, 23] at various conditions [11, 48–58], we can say atomic manner of these structure is important for prediction of nanoparticle aggregation. Today, molecular dynamics (MD) simulation is one of the exact methods to study atomic systems manner. Historically, MD simulations were initially expanded in the late 1950s, following the earlier accomplishments of Monte Carlo simulations [24–26]. Its growth was based on Laplace's foundational work [27]. In 1957, Wainwright and Alder applied a computer for simulating completely elastic collisions between hard structures [28]. In 1960, Gibson and others simulated radiation damage of solid copper by using a Born–Mayer type of repulsive interaction in addition to the united surface force [29]. The landmark simulation of liquid argon, which applied a Lennard-Jones (LJ) potential, was released by Rahman in 1964. Technically, molecular systems contain plenty of particles and determining the features of such complicated systems is not possible. By using numerical methods, MD simulation avoids this problem. Nevertheless, long MD simulations are mathematically inappropriate and they generate a lot of mistakes in numerical integration which could be decreased by appropriate choice of parameters and algorithms, but they could not be omitted completely. This computational approach is applicable to the study of various types of systems. In this work, we used this computational method to study nanofluid manner [59–78], composed of Al₂O₃ nanoparticles in argon fluid in the presence of external magnetic field. Atomic barrier with cone shape to nanofluid medium is a novelty in our computational study which improves or the simulation results and more adapted by reality cases.

Method

MD simulations based on atomic representations are among the most commonly used methods, to investigate nanofluids manner [30–33]. We used MD simulations to calculate the aggregation of hybrid nanoparticles in liquid argon with the first conditions. MD is a computer simulation procedure to trace evolution of molecules and atoms for a period of time. In this way, for each time step, particles can be free for interactions, giving the perception of the mechanical development of the atomic system. In general version of MD simulation, the particle trajectories are settled by solving Newton's equations for the particle systems, at which forces between particles and their possible energies are frequently computed by interatomic force field https://en.wikipedia.org/wiki/Interatomic_potential. The results of the MD simulations are based on selection of interatomic force field. Interatomic interaction between nanofluids atoms in platinum microchannel is accounted by universal force field (UFF) and embedded atom model (EAM) force field [34, 35]. UFF is a whole atom potential having parameters for each atom. These force field parameters are calculated by using usual rules base on the element, its connectivity and hybridization. The philosophy of UFF force field is using general force constant and geometric parameters that are based on simple hybridization considerations instead of individual force constant and geometric parameters which are depended on special atom combinations using in the angle terms. In this force field, LJ potential applied for non-bond interaction between various atoms [36]:

$$\phi(r_{ij}) = 4\epsilon \left[\left(\frac{\sigma}{r_{ij}} \right)^{12} - \left(\frac{\sigma}{r_{ij}} \right)^6 \right] \quad r_{ij} \leq r_c \quad (1)$$

where ϵ is the depth of the potential, σ is the limited distance at which the interatomic potential is zero, and r is the distance between atoms. In this equation, cutoff radius is indicated by r_c (see Table 1 for other constant amounts).

Furthermore, the EAM potential energy of an atom, i , is given by [34, 35]:

$$E_i = F_\alpha \left(\sum_{i \neq j} \rho_\beta(r_{ij}) \right) + \frac{1}{2} \sum_{i \neq j} \phi_{\alpha\beta}(r_{ij}) \quad (2)$$

Table 1 Length and energy of LJ potential [35, 36]

Element	$\sigma/\text{\AA}$	$\epsilon/\text{kcal mol}^{-1}$
Ar	3.868	0.185
Al	4.499	0.505
O	3.500	0.060
Pt	2.754	0.080

The distance between atoms i and j is shown by r_{ij} , $\phi_{\alpha\beta}$ is a pair-wise possible function, $\rho_{\alpha\beta}$ is the contribution to electron charge density from atom j of type β at the place of atom i , and F_{α} is an embedding function which represents the energy that is necessary for placing atom i of type α into the electron cloud. To calculate the particle's movement via simulation time, Newton's second law at the atomic level is used as the gradient of the interatomic potential in Eq. (3),

$$F_i = \sum_{i \neq j} F_{ij} = m_i \frac{d^2 r_i}{dt^2} = m_i \frac{dv_i}{dt} \quad (3)$$

After that, Gaussian distribution is fulfilled for calculating the temperature of particles that is shown in this formula:

$$\frac{3}{2} k_B T = \frac{1}{N_{\text{atom}}} \sum_{i=1}^N \frac{1}{2} m v_i^2 \quad (4)$$

Newton's law:

$$v(t + \delta t) = v(t) + a(t)\delta t \quad (5)$$

$$r(t + \delta t) = r(t) + v(t)\delta t \quad (6)$$

$r(t)$ and $v(t)$ are the initial rates of these mechanical parameters. In our study, every MD simulation was doing by applying Large-scale Atomic/Molecular Massively Parallel Simulator (LAMMPS) simulation package released by Sandia National Laboratories [37–40]. Finally, we can say that our MD simulations were done in two steps:

Step A Argon- Al_2O_3 nanofluid was simulated with atomic details. For this procedure, atomic structure temperature was fixed at 300 K with 1 femtosecond time step and periodic boundary condition implemented in x and y directions and fixed one used for z direction [41]. By definition of initial settings of MD simulations, atomic structure equilibrated for 1 ns. After that, the system reached to equilibrium state and computational running continued to 2 ns. In this step of MD simulation, the potential energy of atomic structures was reported to verify our MD simulations.

Step B In the second step, external magnetic field was inserted to simulation box. The simulated structures equilibrated for 1 ns at 300 K with nose–Hoover thermostat [42, 43]. In our calculations, the temperature damping rate was set to 0.01 rate. Then, the atomic interaction between atoms fulfilled for 2 ns. Finally, to analyze nanoparticle aggregation phenomena, physical parameters such as potential energy, distance of structures, and radial distribution function (RDF) were reported.

Results and discussions

Equilibrium MD consequences

At the first section, not only the atomic structure of non-ideal Pt microchannel and fluid/nanofluid but also the accuracy of atomic structure and used force fields are studied. The length of Pt microchannel in our simulations is $300 \times 300 \times 1000 \text{ \AA}^3$ in x , y and z directions, respectively. Further, Ar/ Al_2O_3 nanofluid is simulated in interior space of simulated microchannel. The atomic structure can be seen in Fig. 1 [44]. In Fig. 1, it should be noted that this figure is related to Ar base fluid in non-ideal microchannel which is depicted in top, front, and perspective views. OVITO is a scientific visualization and analysis package for atomistic and particle-based simulations. Our MD simulations showed that the initial position of atoms in microchannel and fluid/nanofluid structures is adopted with UFF and EAM force fields. Physically, the stability of atomic structures is described by reporting potential energy of these structures at 300 K. Figure 2. shows the potential energy of atomic structures as a function of simulation time. Base on this figure, one can see the atomic structures energy converged after 1 ns simulation and this parameter of base fluid reached to -272 eV .

In this section, atomic structure of microchannel and Ar/ Al_2O_3 nanofluid is studied. Figure 3 shows the simulated nanofluid with various numbers of Al_2O_3 nanoparticles ($N=2, 3$, and 4). Our MD simulations show that the initial position of atoms in nanofluids is adopted with UFF and EAM force fields. The stability of atomic structures is described by reporting potential energy of these structures. Figure 4. shows the possible energy of atomic structures as a function of simulation time. Base on this figure, one can see the atomic structures energy converged after 1 ns simulation to -411 eV , -442 eV , and -470 eV for nanofluid with 2, 3, and 4 nanoparticles, respectively. Numerically, the potential energy value increases by the number of nanoparticles increasing. This manner shows that, by Al_2O_3 nanoparticle adding to Ar fluid, the stability of structure rises. Physically, in atomic structures with negative potential energy, the atoms bonded to each other with attractive atomic force and so we conclude attractive force between nanofluid atoms is bigger than fluid one.

Dynamical evolution of atomic structures

After initial MD simulation and temperature equilibration of Pt microchannel and Ar/ Al_2O_3 nanofluid, external force

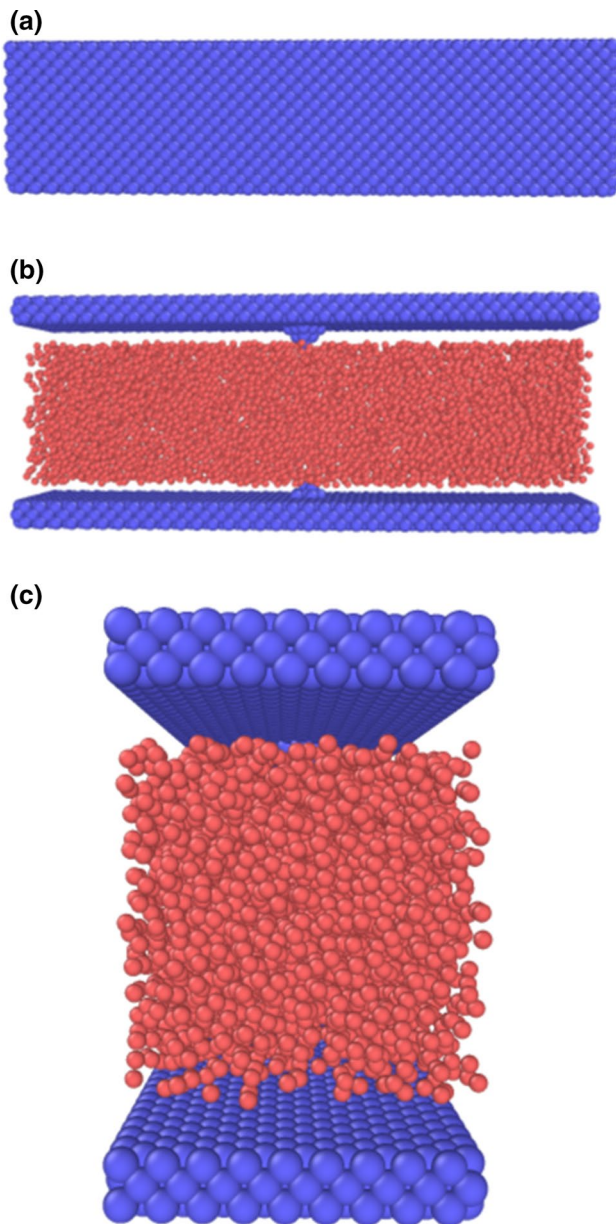


Fig. 1 Schematic of simulated non-ideal platinum microchannel and argon fluid by using the LAMMPS at **a** top, **b** front, and **c** perspective directions

with $0.002 \text{ eV } \text{Å}^{-1}$ magnitude is inserted to nanofluid and micro-canonical ensemble implemented to the next 2 ns. In statistical mechanics, a micro-canonical ensemble is the statistical condition which is used to show the probable states of a mechanical system that contains a completely specified energy. It is supposed that the system is isolated, i.e., it cannot exchange energy or particles with its environment; thus, as time passes, by saving of energy, the energy of the system remains exactly the same. In the first step of this section, we will report the center of mass (COM) distance between

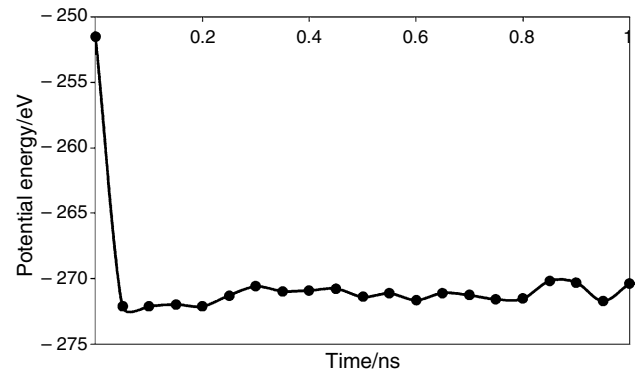


Fig. 2 Potential energy variation of Ar fluid as a function of simulation time

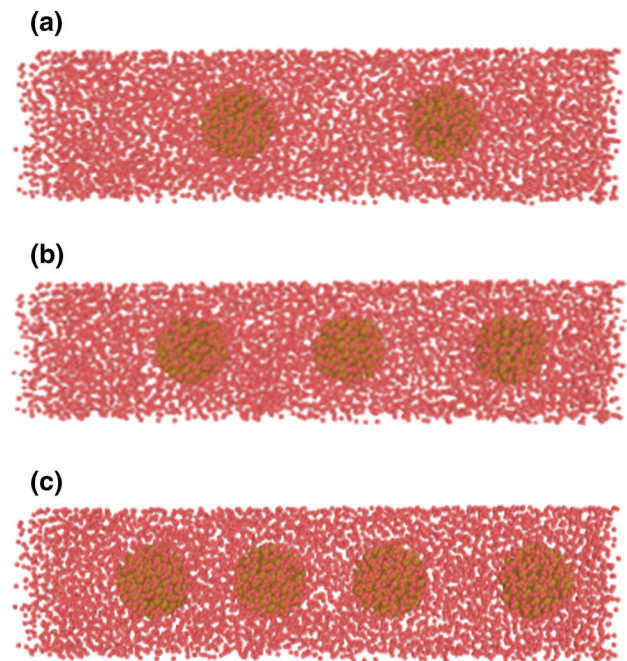


Fig. 3 Atomic representation of the Ar/ Al_2O_3 nanofluid structure with **a** 2, **b** 3, and **c** 4 nanoparticles by using the LAMMPS package

nanoparticles. The center of mass of a distribution of mass in space is the special point that the weighted relative position of the distributed mass reaches to zero [45]. From Fig. 5, we can see that the interatomic force is attractive one and so nanoparticles get closer to each other. Numerically, the distance of nanoparticles varies from 50 to 2.1 Å at 300 K. From Fig. 6 we can see the slope of particles distance is changing non-uniformly. This atomic manner arises from atomic interaction between particles which is described by LJ force field. In this force field, the interatomic force gets positive and negative in various atomic distances. Further, this physical parameter decreases by N increasing

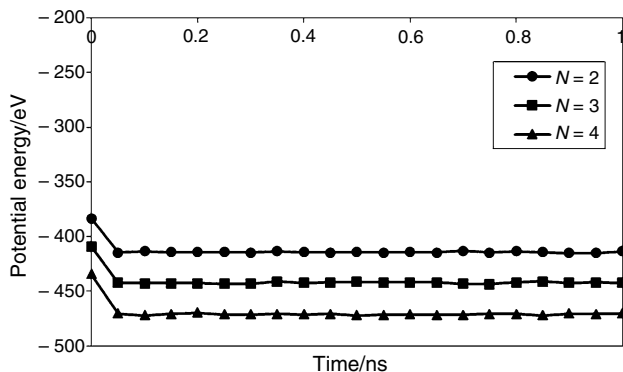


Fig. 4 Potential energy variation of Ar/Al₂O₃ nanofluid according to the simulation time and number of nanoparticles

as reported in Table 2. This manner of atomic structures arises from increasing potential energy and attraction force between Al₂O₃ nanoparticles. Physically, increasing the interatomic force between nanoparticles causes more Al₂O₃ atoms penetration together. In next step, the time-dependent external magnetic field is inserted to Ar/Al₂O₃ nanofluid by the following equation:

$$B = qv\mathbf{B} \sin(\omega t) \tag{7}$$

q is electrical charge, v is atoms velocity, B is magnetic field magnitude, ω is field frequency, and t is the MD simulation time. By adding this magnetic field, the aggregation process occurs in shorter time. In Tables 3 and 4, the time of aggregation phenomena for different simulated structures with time-dependent magnetic field is reported. By more magnitude of external field, the time of aggregation phenomena increases. Furthermore, by increasing frequency, the time of Al₂O₃ nanoparticles aggregation increases and it happens because of atoms fluctuation.

After equilibration procedure of atomic structures, the radial distribution function (RDF) of Al₂O₃ nanoparticles is calculated to investigate the Al₂O₃ aggregation phenomena in non-ideal Pt microchannel. In this step, g(r) is defined as follows [46, 47]:

Fig. 5 Time evolution of Al₂O₃ nanoparticles aggregation in MD simulations

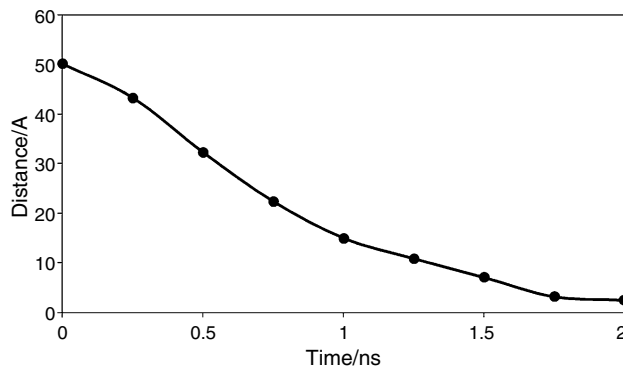
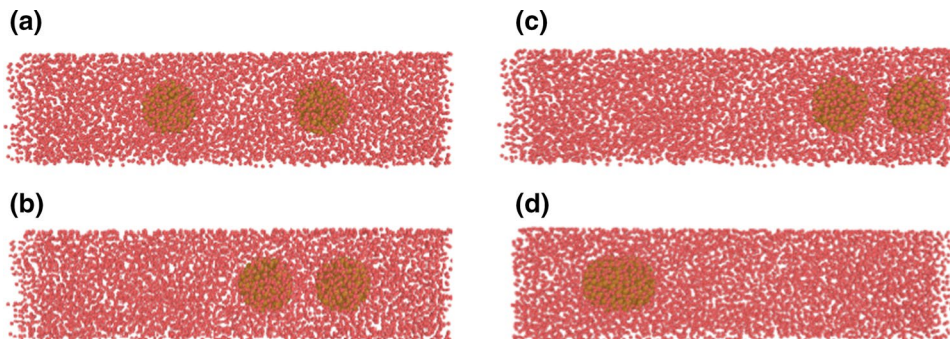


Fig. 6 COM distance variation of Al₂O₃ nanoparticles as a function of simulation time

Table 2 COM distance of Al₂O₃ nanoparticles as a function of simulation time and nanoparticle number without external magnetic field

Al ₂ O ₃ number	COM distance/A	Time/ns
2	2.5	2
3	2.4	1.8
4	2.1	1.7

Table 3 COM distance of Al₂O₃ nanoparticles as a function of simulation time and nanoparticle number with external magnetic field (B=1 and ω=0.1)

Al ₂ O ₃ number	COM distance/A	Time/ns
2	2.6	2.4
3	2.5	2.3
4	2.5	2.3

Table 4 COM distance of Al₂O₃ nanoparticles as a function of B and ω variation at t=1 ns MD simulation

B rate	Ω rate	COM distance/A
1	0.1	2.6
2	0.1	2.9
3	0.1	3.1
1	0.2	2.5
1	0.3	2.7

$$g(r) = \frac{dn_r}{4\pi dr\rho} \quad (8)$$

In this equation, r is the distance between the Al_2O_3 nanoparticles respect to each other. $g(r)$ defines the probability of finding a nanoparticle at a distance r from central nanoparticle. dn_r is a function that computes the number of particles within a shell of thickness dr and ρ is the density of atomic structure. Physically, the radial distribution function is useful to analyze the spheroid distribution of the Al_2O_3 molecules around every nanoparticle since it is normalized by the volume of the spheroid shell. In RDF curve, the distance from the initial atomic structure, at which there is the most possibility to find a neighbor target atom, creates the first peak. It shows the most possible and the closest neighbor distance. Over large radius, the oscillations in $g(r)$ are decreased, and it approaches the value of unity when normalized the mean density. The first and second peak of nanoparticles RDF as a function of various time-dependent magnetic field is reported in Tables 5 and 6. In addition, from Fig. 7a we can see that the attraction force between nanoparticles decreases when \mathbf{B} increases. Further, ω is reciprocal relation with interatomic force between nanoparticles (Fig. 7b). Numerically, the most possible distance to find nanoparticles molecules varies from 1.3 to 1.7 Å by increasing $\mathbf{B} = 1$ to $\mathbf{B} = 3$ and this physical parameter varies from 1.3 to 1.8 Å by increasing $w = 0.1$ to $w = 0.4$. This manner of atomic structures arises from decreasing the amplitude of the atomic fluctuations by b/w increasing. Finally, increasing the amplitude of atomic fluctuation causes decreasing penetration of atoms to each other and so the aggregation of nanoparticles in simulated nanofluids occurs in bigger simulation time. This manner of nanofluids which reported in this section can be used in heat transfer applications to improve their efficiency.

Table 5 Position of the first and second peak of Al_2O_3 nanoparticle's RDF as a function of \mathbf{B} magnitude of external magnetic field

B magnitude	First peak/Å	Second peak/Å
1	1.3	1.9
2	1.5	2.1
3	1.7	2.3

Table 6 Position of the first and second peak of Al_2O_3 nanoparticle's RDF as a function of ω rate of external magnetic field

ω	First peak/Å	Second peak/Å
0.1	1.3	2.0
0.2	1.6	2.2
0.3	1.8	2.4

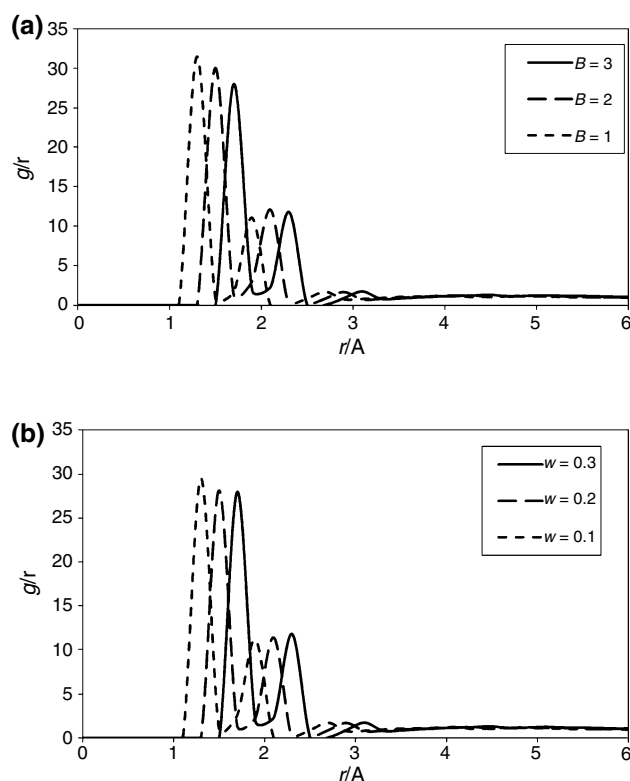


Fig. 7 Radial distribution function of Al atoms as a function of sample **a** \mathbf{B} and **b** ω parameters of external magnetic field

Conclusions

We used the molecular dynamics method for simulating the aggregation process of hybrid nanoparticles which is inserted to Ar base fluid in non-ideal microchannel with pyramidal barriers. Our computational results from atomic simulations are as follows:

- Universal force field and embedded atom model force field are the suitable interatomic potential to simulation of nanofluid atomic structures.
- By increasing nanoparticles into liquid Argon, the stability of nanofluid increases and potential energy of these structures raises to -470 eV from -272 eV.
- Al_2O_3 center of mass decreases by time passing in our simulations from 50 Å to 2.1 Å in which, by the optimal magnetic field inserting to nanofluid, this parameter changes to 2.7 Å.
- Generally, increasing amplitude and frequency of external magnetic field leads to the aggregation delay of nanoparticles and these phenomenon occur after 2.3 ns.
- Involving the optimal magnetic field, the first peak of this atomic structure radial distribution function varies from 1.3 to 1.8 Å.

These numerical results from our computational study can be used in industry for the design of new heat transfer apparatus.

References

- Taylor RA, et al. Small particles, big impacts: a review of the diverse applications of nanofluids. *J Appl Phys.* 2013;113(1):011301. <https://doi.org/10.1063/1.4754271>.
- Buongiorno J. Convective transport in nanofluids. *J Heat Transf.* 2006;128(3):240–50. <https://doi.org/10.1115/1.2150834>.
- Das SK, Choi SU, Yu W, Pradeep T. *Nanofluids: science and technology.* Hoboken: Wiley-Interscience; 2007. p. 397.
- Kakaç Sadik, Pramuanjaroenkij Anchasa. Review of convective heat transfer enhancement with nanofluids. *Int J Heat Mass Transf.* 2009;52(13–14):3187–96. <https://doi.org/10.1016/j.ijheatmasstransfer.2009.02.006>.
- Witharana S, Chen H, Ding Y. Stability of nanofluids in quiescent and shear flow fields. *Nanoscale Res Lett.* 2011;6:231.
- Sajid MU, Ali HM. Thermal conductivity of hybrid nanofluids: a critical review. *Int J Heat Mass Transf.* 2018;126:211–34. <https://doi.org/10.1016/j.ijheatmasstransfer.2018.05.021>.
- Babar Hamza, Sajid Muhammad Usman, Ali Hafiz. Viscosity of hybrid nanofluids: a critical review. *Therm Sci.* 2019;23:15. <https://doi.org/10.2298/TSCI181128015B>.
- Sajid MU, Ali HM. Recent advances in application of nanofluids in heat transfer devices: a critical review. *Renew Sustain Energy Rev.* 2019;103:556–92. <https://doi.org/10.1016/j.rser.2018.12.057>.
- Chen H, Witharana S, et al. Predicting thermal conductivity of liquid suspensions of nanoparticles (nanofluids) based on rheology. *Particuology.* 2009;7(2):151–7. <https://doi.org/10.1016/j.partic.2009.01.005>.
- Sajid MU, Ali HM, Sufyan A, Rashid D, Zahid SU, Rehman WU. Experimental investigation of TiO₂–water nanofluid flow and heat transfer inside wavy mini-channel heat sinks. *J Therm Anal Calorim.* 2019. <https://doi.org/10.1007/s10973-019-08043-9>.
- Wahab A, Hassan A, Qasim MA, Ali HM, Babar H, Sajid MU. Solar energy systems–potential of nanofluids. *J Mol Liq.* 2019;289:111049. <https://doi.org/10.1016/j.molliq.2019.111049>.
- Sarafraz MM, Tlili I, Abdul Baseer M, Safaei MR. Potential of solar collectors for clean thermal energy production in smart cities using nanofluids: experimental assessment and efficiency improvement. *Appl Sci.* 2019;9(9):1877. <https://doi.org/10.3390/app9091877>.
- Sarafraz MM, Peyghambarzadeh SM. Experimental study on subcooled flow boiling heat transfer to water–diethylene glycol mixtures as a coolant inside a vertical annulus. *Exp Therm Fluid Sci.* 2013;50:154–62. <https://doi.org/10.1016/j.expthermflusci.2013.06.003>.
- Forrester DM, et al. Experimental verification of nanofluid shear-wave reconversion in ultrasonic fields. *Nanoscale.* 2016;8(10):5497–506. <https://doi.org/10.1039/c5nr07396k>.
- Kuznetsov AV, Nield DA. Natural convective boundary-layer flow of a nanofluid past a vertical plate. *Int J Therm Sci.* 2010;49(2):243–7. <https://doi.org/10.1016/j.ijthermalsci.2009.07.015>.
- Wasan DT, Nikolov AD. Spreading of nanofluids on solids. *Nature.* 2003;423(6936):156–9. <https://doi.org/10.1038/nature01591>.
- Das SK. Heat transfer in nanofluids—a review. *Heat Transfer Eng.* 2006;27(10):3–19. <https://doi.org/10.1080/01457630600904593>.
- Azwadi Nor, Sidik Che. A review on preparation methods and challenges of nanofluids. *Int Commun Heat Mass Transf.* 2014;54:115–25. <https://doi.org/10.1016/j.icheatmasstransfer.2014.03.002>.
- Nkurikiyimfura I, Wang Y, Pan Z. Effect of chain-like magnetite nanoparticle aggregates on thermal conductivity of magnetic nanofluid in magnetic field. *Exp Therm Fluid Sci.* 2013;44:607–12.
- Xuan Y, Li Q, Hu W. Aggregation structure and thermal conductivity of nanofluids. *AIChE J.* 2003;49:1038–43.
- Murshed SMS, Leong KC, Yang C. Enhanced thermal conductivity of TiO₂–water based nanofluids. *Int J Therm Sci.* 2005;44:367–73.
- Song D, Jing D, Geng J, et al. A modified aggregation based model for the accurate prediction of particle distribution and viscosity in magnetic nanofluids. *Powder Technol.* 2015;283:561–9.
- Duan F, Kwek D, Crivoi A. Viscosity affected by nanoparticle aggregation in Al₂O₃–water nanofluids. *Nanoscale Res Lett.* 2011;6:248.
- Fermi E, Pasta J, Ulam S. Los alamos report la-1940. *Fermi Collect Pap.* 1955;2:977–88.
- Alder BJ, Wainwright TE. Studies in molecular dynamics. I. General method. *J. Chem. Phys.* 1959;31(2):459. <https://doi.org/10.1063/1.1730376>.
- Rahman A. Correlations in the motion of atoms in liquid argon. *Phys Rev.* 1964;136(2A):A405–11. <https://doi.org/10.1103/physrev.136.a405>.
- de Laplace PS. *Oeuvres Completes de Laplace, Theorie Analytique des Probabilites.* Paris: Gauthier-Villars; 1820 (in French).
- Mesirov JP, Schulten K, Sumners DW, editors. *Mathematical approaches to biomolecular structure and dynamics. The IMA volumes in mathematics and its applications, vol. 82.* New York: Springer-Verlag; 1996. p. 218–47. ISBN 978-0-387-94838-6.
- Gibson JB, Goland AN, Milgram M, Vineyard GH. Dynamics of radiation damage. *Phys Rev.* 1960;120(4):1229–53. <https://doi.org/10.1103/physrev.120.1229>.
- Achhal EM, Jabraoui H, Zeroual S, Loulijat H, Hasnaoui A, Ouaskit S. Modeling and simulations of nanofluids using classical molecular dynamics: particle size and temperature effects on thermal conductivity. *Adv Powder Technol.* 2018;29(10):2434–9. <https://doi.org/10.1016/j.apt.2018.06.023>.
- Jabbari F, Saedodin S, Rajabpour A. Experimental investigation and molecular dynamics simulations of viscosity of CNT-water nanofluid at different temperatures and volume fractions of nanoparticles. *J Chem Eng Data.* 2018. <https://doi.org/10.1021/acs.jced.8b00783>.
- Bao L, Zhong C, Jie P, Hou Y. The effect of nanoparticle size and nanoparticle aggregation on the flow characteristics of nanofluids by molecular dynamics simulation. *Adv Mech Eng.* 2019;11(11):168781401988948. <https://doi.org/10.1177/1687814019889486>.
- Kang H, Zhang Y, Yang M, Li L. Molecular dynamics simulation of thermal conductivity and viscosity of a nanofluid: effect of nanoparticle aggregation. Volume 10: heat and mass transport processes, parts A and B. 2011. <https://doi.org/10.1115/imece2011-62297>.
- Rappe AK, Casewit CJ, Colwell KS, Goddard WA III, Skif WM. UFF, a full periodic table force field for molecular mechanics and molecular dynamics. *J Am Chem Soc.* 1992;114:10024–35.
- Daw MS, Baskes MI. Embedded-atom method: derivation and application to impurities, surfaces, and other defects in metals. *Phys Rev B.* 1984;29(12):6443–53. <https://doi.org/10.1103/physrevb.29.6443>.
- Lennard-Jones JE. On the determination of molecular fields. *Proc R Soc Lond A.* 1924;106(738):463–77. <https://doi.org/10.1098/rspa.1924.0082>.

37. Plimpton S. Fast parallel algorithms for short-range molecular dynamics. *J Comput Phys.* 1995;117(1):1–19. <https://doi.org/10.1006/jcph.1995.1039>.
38. Plimpton SJ, Thompson AP. Computational aspects of many-body potentials. *MRS Bull.* 2012;37(05):513–21. <https://doi.org/10.1557/mrs.2012.96>.
39. Brown WM, Wang P, Plimpton SJ, Tharrington AN. Implementing molecular dynamics on hybrid high performance computers—short range forces. *Comput Phys Commun.* 2011;182(4):898–911. <https://doi.org/10.1016/j.cpc.2010.12.021>.
40. Brown WM, Kohlmeyer A, Plimpton SJ, Tharrington AN. Implementing molecular dynamics on hybrid high performance computers—particle–particle particle–mesh. *Comput Phys Commun.* 2012;183(3):449–59. <https://doi.org/10.1016/j.cpc.2011.10.012>.
41. Mai W, Li P, Bao H, Li X, Jiang L, Hu J, Werner DH. Prism-based DGTD with a simplified periodic boundary condition to analyze FSS with D2n symmetry in a rectangular array under normal incidence. *IEEE Antennas Wirel Propag Lett.* 2019;18(4):771–5. <https://doi.org/10.1109/LAWP.2019.2902340> ISSN 1536-1225.
42. Nosé S. A unified formulation of the constant temperature molecular-dynamics methods. *J Chem Phys.* 1984;81(1):511–9. <https://doi.org/10.1063/1.447334>.
43. Hoover WG. Canonical dynamics: equilibrium phase-space distributions. *Phys Rev A.* 1985;31(3):1695–7. <https://doi.org/10.1103/physreva.31.1695>.
44. Stukowski A. Visualization and analysis of atomistic simulation data with OVITO—the open visualization tool. *Model Simul Mater Sci Eng.* 2009;18(1):015012. <https://doi.org/10.1088/0965-0393/18/1/015012>.
45. Beatty MF. Principles of engineering mechanics, volume 2: dynamics—the analysis of motion, mathematical concepts and methods in science and engineering, vol. 33. Berlin: Springer; 2006. ISBN 978-0-387-23704-6.
46. Dinnebier RE, Billinge SJL. Powder diffraction: theory and practice. 1st ed. Cambridge: Royal Society of Chemistry; 2008. p. 470–3. <https://doi.org/10.1039/9781847558237>. ISBN 978-1-78262-599-5.
47. Hansen JP, McDonald IR. Theory of simple liquids. 3rd ed. Cambridge: Academic Press; 2005.
48. Sarafraz MM, Safaei MR. Diurnal thermal evaluation of an evacuated tube solar collector (ETSC) charged with graphene nanoplatelets-methanol nano-suspension. *Renew Energy.* 2019;142:364–72.
49. Goodarzi H, Akbari OA, Sarafraz MM, Karchegani MM, Safaei MR, Sheikh Shabani GA. Numerical simulation of natural convection heat transfer of nanofluid with Cu, MWCNT, and Al₂O₃ nanoparticles in a cavity with different aspect ratios. *J Thermal Sci Eng Appl.* 2019;11(6):061020.
50. Sarafraz MM, Safaei MR, Tian Z, Goodarzi M, Bandarra Filho EP, Arjomandi M. Thermal assessment of nano-particulate graphene-water/ethylene glycol (WEG 60: 40) nano-suspension in a compact heat exchanger. *Energies.* 2019;12(10):1929.
51. Pourmehran O, Sarafraz MM, Rahimi-Gorji M, Ganji DD. Rheological behaviour of various metal-based nano-fluids between rotating discs: a new insight. *J Taiwan Inst Chem Eng.* 2018;88:37–48.
52. Salari E, Peyghambarzadeh SM, Sarafraz MM, Hormozi F, Nikkha V. Thermal behavior of aqueous iron oxide nano-fluid as a coolant on a flat disc heater under the pool boiling condition. *Heat Mass Transf.* 2017;53(1):265–75.
53. Sarafraz MM, Hormozi F, Kamalgharibi M. Sedimentation and convective boiling heat transfer of CuO–water/ethylene glycol nanofluids. *Heat Mass Transf.* 2014;50(9):1237–49.
54. Sarafraz MM, Arjomandi M. Thermal performance analysis of a microchannel heat sink cooling with copper oxide-indium (CuO/In) nano-suspensions at high-temperatures. *Appl Therm Eng.* 2018;137:700–9.
55. Sarafraz MM, Arjomandi M. Demonstration of plausible application of gallium nano-suspension in microchannel solar thermal receiver: experimental assessment of thermo-hydraulic performance of microchannel. *Int Commun Heat Mass Transfer.* 2018;94:39–46.
56. Sarafraz MM, Arya H, Arjomandi M. Thermal and hydraulic analysis of a rectangular microchannel with gallium-copper oxide nano-suspension. *J Mol Liq.* 2018;263:382–9.
57. Soudagar MEM, Kalam MA, Sajid MU, Afzal A, Banapurmath NR, Akram N, Mane SD, Saleel CA. Thermal analyses of minichannels and use of mathematical and numerical models. *Numer Heat Transf Part A: Appl.* 2020;77(5):497–537.
58. Sajid MU, Ali HM, Sufyan A, Rashid D, Zahid SU, Rehman WU. Experimental investigation of TiO₂–water nanofluid flow and heat transfer inside wavy mini-channel heat sinks. *J Therm Anal Calorim.* 2019;137(4):1279–94.
59. Torabi M, Hamed A, Alamatian E, Zahabi H. The effect of geometry parameters and flow characteristics on erosion and sedimentation in channel’s junction using finite volume method. *Int J Eng Manag Res.* 2019;9:115–23.
60. Olia H, Torabi M, Bahiraei M, Ahmadi MH, Goodarzi M, Safaei MR. Application of nanofluids in thermal performance enhancement of parabolic trough solar collector: state-of-the-art. *Appl Sci.* 2019;9(3):463.
61. Zahabi H, Torabi M, Alamatian E, Bahiraei M, Goodarzi M. Effects of geometry and hydraulic characteristics of shallow reservoirs on sediment entrapment. *Water.* 2018;10(12):1725.
62. Chero E, Torabi M, Zahabi H, Ghafoorisadatieh A, Bina K. Numerical analysis of the circular settling tank. *Drink Water Eng Sci.* 2019;12(2):39–44.
63. Hosseini D, Torabi M, Moghadam MA. Preference assessment of energy and momentum equations over 2D-SKM method in compound channels. *J Water Resour Eng Manag.* 2019;6(1):24–34.
64. Alrashed AA, Akbari OA, Heydari A, Toghraie D, Zarringhalam M, Shabani GAS, Seifi AR, Goodarzi M. The numerical modeling of water/FMWCNT nanofluid flow and heat transfer in a backward-facing contracting channel. *Physica B.* 2018;537:176–83.
65. Bahmani MH, Sheikhzadeh G, Zarringhalam M, Akbari OA, Alrashed AA, Shabani GAS, Goodarzi M. Investigation of turbulent heat transfer and nanofluid flow in a double pipe heat exchanger. *Adv Powder Technol.* 2018;29(2):273–82.
66. Alrashed AA, Gharibdousti MS, Goodarzi M, de Oliveira LR, Safaei MR, Bandarra Filho EP. Effects on thermophysical properties of carbon based nanofluids: experimental data, modelling using regression, ANFIS and ANN. *Int J Heat Mass Transf.* 2018;125:920–32.
67. Goodarzi M, D’Orazio A, Keshavarzi A, Mousavi S, Karimipour A. Develop the nano scale method of lattice Boltzmann to predict the fluid flow and heat transfer of air in the inclined lid driven cavity with a large heat source inside, Two case studies: pure natural convection & mixed convection. *Physica A.* 2018;509:210–33.
68. Gheynani AR, Akbari OA, Zarringhalam M, Shabani GAS, Alnaqi AA, Goodarzi M, Toghraie D. Investigating the effect of nanoparticles diameter on turbulent flow and heat transfer properties of non-Newtonian carboxymethyl cellulose/CuO fluid in a micro-tube. *Int J Numer Methods Heat Fluid Flow.* 2019;29:1699–723.
69. Pordanjani AH, Aghakhani S, Karimipour A, Afrand M, Goodarzi M. Investigation of free convection heat transfer and entropy generation of nanofluid flow inside a cavity affected by magnetic field and thermal radiation. *J Therm Anal Calorim.* 2019;137(3):997–1019.
70. Bahiraei M, Jamshidmofid M, Goodarzi M. Efficacy of a hybrid nanofluid in a new microchannel heat sink equipped with both secondary channels and ribs. *J Mol Liq.* 2019;273:88–98.
71. Goodarzi M, Toghraie D, Reiszadeh M, Afrand M. Experimental evaluation of dynamic viscosity of ZnO–MWCNTs/engine oil

- hybrid nanolubricant based on changes in temperature and concentration. *J Therm Anal Calorim.* 2019;136(2):513–25.
72. Qureshi ZA, Ali HM, Khushnood S. Recent advances on thermal conductivity enhancement of phase change materials for energy storage system: a review. *Int J Heat Mass Transf.* 2018;127:838–56.
73. Mahbubul IM, Khan MMA, Ibrahim NI, Ali HM, Al-Sulaiman FA, Saidur RJRE. Carbon nanotube nanofluid in enhancing the efficiency of evacuated tube solar collector. *Renew Energy.* 2018;121:36–44.
74. Ali HM, Babar H, Shah TR, Sajid MU, Qasim MA, Javed S. Preparation techniques of TiO_2 nanofluids and challenges: a review. *Appl Sci.* 2018;8(4):587.
75. Ghasemi A, Hassani M, Goodarzi M, Afrand M, Manafi S. Appraising influence of COOH-MWCNTs on thermal conductivity of antifreeze using curve fitting and neural network. *Phys A Stat Mech Appl.* 2019;514:36–45.
76. Moradikazerouni A, Hajizadeh A, Safaei MR, Afrand M, Yarmand H, Zulkifli NWBM. Assessment of thermal conductivity enhancement of nano-antifreeze containing single-walled carbon nanotubes: optimal artificial neural network and curve-fitting. *Phys A Stat Mech Appl.* 2019;521:138–45.
77. Peng Y, Parsian A, Khodadadi H, Akbari M, Ghani K, Goodarzi M, Bach Q-V. Develop optimal network topology of artificial neural network (AONN) to predict the hybrid nanofluids thermal conductivity according to the empirical data of Al_2O_3 -Cu nanoparticles dispersed in ethylene glycol. *Physica A.* 2020;549:124015. <https://doi.org/10.1016/j.physa.2019.124015>.
78. Li ZX, Renault FL, Gómez AOC, Sarafraz MM, Khan H, Safaei MR, Filho EPB. Nanofluids as secondary fluid in the refrigeration system: experimental data, regression, ANFIS, and NN modeling. *Int J Heat Mass Transf.* 2019;144:118635. <https://doi.org/10.1016/j.ijheatmasstransfer.2019.118635>.

Publisher's Note Springer Nature remains neutral with regard to jurisdictional claims in published maps and institutional affiliations.